Biomaterials 31 (2010) 5072–5082

Contents lists available at ScienceDirect

Biomaterials

journal homepage: www.elsevier.com/locate/biomaterials

The influence of hierarchical hybrid micro/nano-textured titanium surface with titania nanotubes on osteoblast functions

Lingzhou Zhao [a,b], Shenglin Mei [a], Paul K. Chu [b,*], Yumei Zhang [a,**], Zhifen Wu [a,***]

[a] School of Stomatology, The Fourth Military Medical University, No. 145 West Changle Road, Xi'an 710032, China
[b] Department of Physics & Materials Science, City University of Hong Kong, Tat Chee Avenue, Kowloon, Hong Kong, China

ARTICLE INFO

Article history:
Received 22 December 2009
Accepted 8 March 2010
Available online 2 April 2010

Keywords:
Titania
Osseointegration
Osteoblast
Nanotubes
Microtopography

ABSTRACT

Hierarchical hybrid micro/nano-textured titanium surface topographies with titania nanotubes were produced by simple acid etching followed by anodization to mimic the hierarchical structure of bone tissues. Primary rat osteoblasts were used to evaluate the bioactivity. The microtopography formed by acid etching of titanium induced inconsistent osteoblast functions with initial cell adhesion and osteogenesis-related gene expression being dramatically enhanced while other cell behaviors such as proliferation, intracellular total protein synthesis and alkaline phosphatase activity, collagen secretion, and extracellular matrix mineralization being depressed. In comparison, addition of nanotubes to the microtopography led to enhancement of multiple osteoblast functions. Nearly all the cell functions investigated in this study were retained or promoted. Compared to a microtopography, the enhancement of multiple cell functions observed from the hierarchical micro/nano-textured surfaces is expected to lead to faster bone maturation around the titanium implants without compromising the bone mass. In addition, the hierarchical micro/nano-textured surfaces still retain the mechanical interlocking ability of the microtopography thereby boding well for osseointegration. Our study reveals a synergistic role played by the micro and nanotopographies in osteoblast functions and provides insight to the design of better biomedical implant surfaces.

1. Introduction

It is well known that the surface characteristics of biomedical implants play critical roles in cell or extracellular matrix interactions with the implants and eventual osseointegration [1]. The interactions between cells and microtopographies have been extensively studied. It has been suggested that microtopographies can promote bone-to-implant contact via such mechanisms as mechanical interlocking [2] and enhancement of osteoblast functions by these microtopographies [3,4]. Some microtopographies have already been adopted on commercial implant products and good clinical performance has been obtained on hydrofluoric (HF) acid treated titanium implants [5–7]. However, microrough surfaces depress osteoblast proliferation though they are effective in promoting osteoblast differentiation [8–12], resulting in a smaller bone mass accumulated compared to a smooth surface.

The interactions between cells and nanotopographies are of increasing interest as a nanotopographies may be more efficient in promoting cell functions [13] and titania nanotubes have attracted much attention [14–33]. Titania nanotubes can be fabricated easily with precisely controlled diameters and lengths. Titania nanotubes with the suitable tube dimensions have been observed to enhance bone cell functions [14,15,17,19,20,22,24,25,27], even though there is still some controversy. These nanotubes can also serve as carriers for drugs such as growth factors [30,31], antibacterial agents [15,19] and other drugs [31] and show promise in bone implant applications.

Natural tissues are hierarchical structures assembled in a highly organized way composed of nano-, micro-, and macro-scale building blocks, of which bone tissues constitute a good example. Bone tissues are composed of nanostructures including non-collageneous organic proteins, fibrillar collagen and hydroxyapatite crystals, microstructures including lamellae, osteons and Haversian systems, as well as macrostructures such as cancellous and cortical bones [34]. From the biomimetic viewpoint, a hierarchical structure composed of micro- and nanoscale components may provide a more suitable surface topography for cell functions as it can better mimic the structure of the natural extracellular matrix. There have been some attempts to fabricate such micro/nanostructures for biomedical applications such as tissue engineering scaffolds [35–38], implant surfaces

* Corresponding author. Tel.: +852 34427724; fax: +852 27889549.
** Corresponding author. Tel.: +86 29 8477 6090; fax: +86 29 8477 6096.
*** Corresponding author. Tel.: +86 29 8477 6093; fax: +86 29 8477 6096.
E-mail addresses: paul.chu@cityu.edu.hk (P.K. Chu), wqtzym@fmmu.edu.cn (Y. Zhang), wzfwxy@fmmu.edu.cn (Z. Wu).

0142-9612/$ – see front matter © 2010 Elsevier Ltd. All rights reserved.
doi:10.1016/j.biomaterials.2010.03.014

[39–41], as well as blood-contacting materials [42]. Tan et al. have produced micro- and nanoscale structures by depositing nano-structured hydroxyapatite on a microscale architecture created by microfabrication technology and these structures enhances some selective cellular functions [37]. Kubo and coworkers developed a micropit-and-nanonodule hybrid titania topography on the titanium surface which enhanced the attachment, spreading, adhesion, proliferation, and differentiation of osteoblasts [39]. Gao et al. fabricated a micro/nanostructured porous surface on titanium and observed increased hydroxyapatite formation in simulated body fluids and faster bovine serum albumin (BSA) adsorption [40]. However, the exact role played by the micro and nanotopographies is still unclear and it is still challenging to produce hierarchical structures that can be directly used clinically.

In this study, biomimetic hierarchical micro/nano-textured surface topographies were produced on titanium by acid etching to produce micropits and subsequent anodization to form a nanotubular layer in order to better mimic the hierarchical structure of bone tissues. As the fabrication method is easy and cost-effective and the mechanical strength of the coatings can be tailored to meet the requirements demanded by biomedical implants, these coatings have high potential. The bioactivity of the materials was evaluated *in vitro* using primary osteoblasts. This study provides insight to the role of the micro and nanotopographies on cell functions.

2. Materials and methods

2.1. Specimen preparation

Pure titanium ($10 \times 10 \times 1$ mm^3) was used as the substrate. After polishing and ultrasonic cleaning, the substrates were treated with 0.5 wt.% HF acid for 30 min, immediately rinsed with distilled water, and dried. They were anodized for 30 min in an electrolyte containing 0.5 wt.% HF acid using a DC power supply with a platinum electrode as the cathode. Two different voltages were chosen to form two typical nano textures (Fig. 1). Immediately after anodization, the samples were rinsed with deionized water. After ultrasonic cleaning, all the samples, including the two hierarchical micro/nano-textured surfaces, namely acid-etched/anodized at 5 V (R-5) and acid-etched/anodized at 20 V (R-20) as well as acid-etched micro-structured surface (R) and polished smooth surface (S), were annealed at 450 °C for 1 h and ultrasonically cleaned. They were sterilized by ultraviolent irradiation for 30 min and polystyrene was used as the control.

2.2. Surface characterization

Field-emission scanning electron microscopy (JSM-6700F, JEOL) was utilized to observe the surface topography of the prepared specimens. Contact angle measurements were carried out by the sessile-drop method on the EasyDrop Standard, KRUSS, Germany at room temperature. Two different liquids, ultrapure water and diiodomethane, were employed in the contact angle measurements. The contact angle θ was measured by analyzing the drop shape using the DSA1 software (KRUSS). The contact angles measured using the two liquids were used to calculate the free energy (SFE) of each surface.

2.3. Protein adsorption assay

A 1 ml droplet of the Dulbecco's minimum essential medium (DMEM, Gibco) containing 10% bovine calf serum (BCS, Gibco) was introduced onto each specimen by a pipet. After incubation for 4 h at 37 °C, the samples were transferred to a new 24-well plate (one disk per well) and washed thrice with 1000 μl PBS. 500 μl of 1% sodium dodecyl sulfate (SDS) solution were added to these wells and shaken for 1 h to detach proteins from the disk surfaces. The protein concentrations in the collected SDS solutions were determined using a MicroBCA protein assay kit (Pierce).

2.4. Cell culture

Primary rat calvarial osteoblasts were obtained by digestion of the calvarial bone of one day old Sprague–Dawley rats [4]. Cells were cultured in DMEM supplemented with 10% BCS and 1% penicillin/streptomycin and incubated in a humidified atmosphere of 5% CO_2 at 37 °C. Passages 2–5 were used.

2.5. Lactate dehydrogenase activity assay

The lactate dehydrogenase (LDH) activity was used as an index of the cytotoxicity in the culture media. After 24 h, the culture media were collected and centrifuged and the supernatant was used for the LDH activity assay. The LDH activity was determined spectrophotometrically according to the manufacturer's instructions.

2.6. Cell adhesion

Osteoblasts were seeded on the substrates at a density of 17 500 cells/cm^2 and allowed to attach for 30, 60, and 120 min. At each prescribed time point, the non-adherent cells were removed by rinsing with phosphate buffered saline (PBS) solution. Cells were fixed and stained with 4′,6′-diamidino-2-phenylindole (DAPI). The cell numbers in five random fields were counted under a fluorescence microscope.

2.7. Cell proliferation

A 1 ml of cell suspension was seeded onto each specimen at a density of 2×10^4 cells/ml and then cultured in DMEM with 10% BCS. After 1, 4 and 7 days, cell proliferation was assessed using a 3-(4,5-dimethylthiazol-2-yl)-2,5-diphenyltetrazolium bromide (MTT) assay. At the prescribed time points, the specimens were gently rinsed three times with PBS and transferred to a new 24-well plate. The MTT solution was added and the specimens were incubated at 37 °C to form formazen, which was then dissolved using dimethyl sulfoxide (DMSO). The optical density (OD) was measured at 490 nm using a spectrophotometer (Bio-tek).

2.8. Intracellular total protein synthesis and alkaline phosphatase activity

The cells were seeded on the specimens in the 24-well plates at a density of 2×10^4 cells/well. After 7 days of culturing, the cells were washed three times with PBS and lysed in 0.1 vol.% Triton X-100 through four standard freeze-thaw cycles. The alkaline phosphatase (ALP) activities of the samples were determined by a colorimetric assay using an ALP reagent containing p-nitrophenyl phosphate (p-NPP) as the substrate. The absorbance of p-nitrophenol formed was measured at a wavelength of 405 nm. The intracellular total protein content was determined using the MicroBCA protein assay kit and the ALP activity was normalized to the total protein content.

2.9. Collagen secretion

Collagen secretion on the specimens was quantified by Sirius Red staining. Cells with a concentration of 2×10^4/well were cultured for 7 days then washed three times with PBS and fixed in 4% paraformaldehyde. Following three rinses in PBS, the constructs were stained for collagen secretion in a 0.1% solution of Sirius Red (Sigma) in saturated picric acid for 18 h. After washing with 0.1 M acetic acid until the red color disappeared, images were taken. In the quantitative analysis, the stain on specimens was eluted in 500 ml of the destain solution (0.2 M NaOH/methanol 1:1). The optical density at 540 nm was then measured using a spectrophotometer.

2.10. Matrix mineralization

Matrix mineralization by primary osteoblasts was evaluated by Alizarin Red staining. After culturing for 7 days, the cells were washed thrice with PBS and then fixed in 75% ethanol for 1 h. The cell cultures were stained with 40 mM Alizarin Red in distilled water (pH 4.2) for 10 min at room temperature. Afterwards, the cell monolayers were washed with distilled water until no more color appearing and then images were acquired. In the quantitative analysis, the stain was dissolved in 10% cetylpyridinum chloride in 10 mM sodium phosphate (pH 7) and the absorbance values were measured at 620 nm.

2.11. Osteogenesis-related gene expressions

The expressions of osteogenisis-related genes were evaluated using the real-time polymerase chain reaction (Real-time PCR). The cells were seeded with 2×10^4 cells/well and cultured for 3 and 10 days. The total RNA was isolated using the TRIzol reagent (Gibco). 1 μg RNA from each sample was reversed transcribed into complementary DNA (cDNA) using the PrimeScript™ RT reagent kit (TaKaRa). The forward and reverse primers for the selected genes were the same as those described in reference [43]. Expressions of osteogenesis-related genes including integrin-β1 (ITG), runt-related transcription factor 2 (RUNX2), ALP, bone morphogenetic protein-2 (BMP), osteopontin (OPN) and osteocalcin (OCN) were quantified using Real-time PCR (Bio-Rad iQ™5 Multicolor Real-Time PCR Detection System) with SYBR® Premix Ex™ Taq II (TaKaRa). Data analysis was carried out using the iQ™5 Optical System Software Version 2.0 (Bio-Rad). The relative expression levels for each gene of interest were normalized to that of the housekeeping gene GAPDH.

2.12. Statistical analysis

The data were analyzed using SPSS 14.0 software (SPSS, USA). A one-way ANOVA followed by a Student-Newman-Keuls *post hoc* test was used to determine the level of significance. $p < 0.05$ was considered to be significant and $p < 0.01$ was considered to be highly significant.

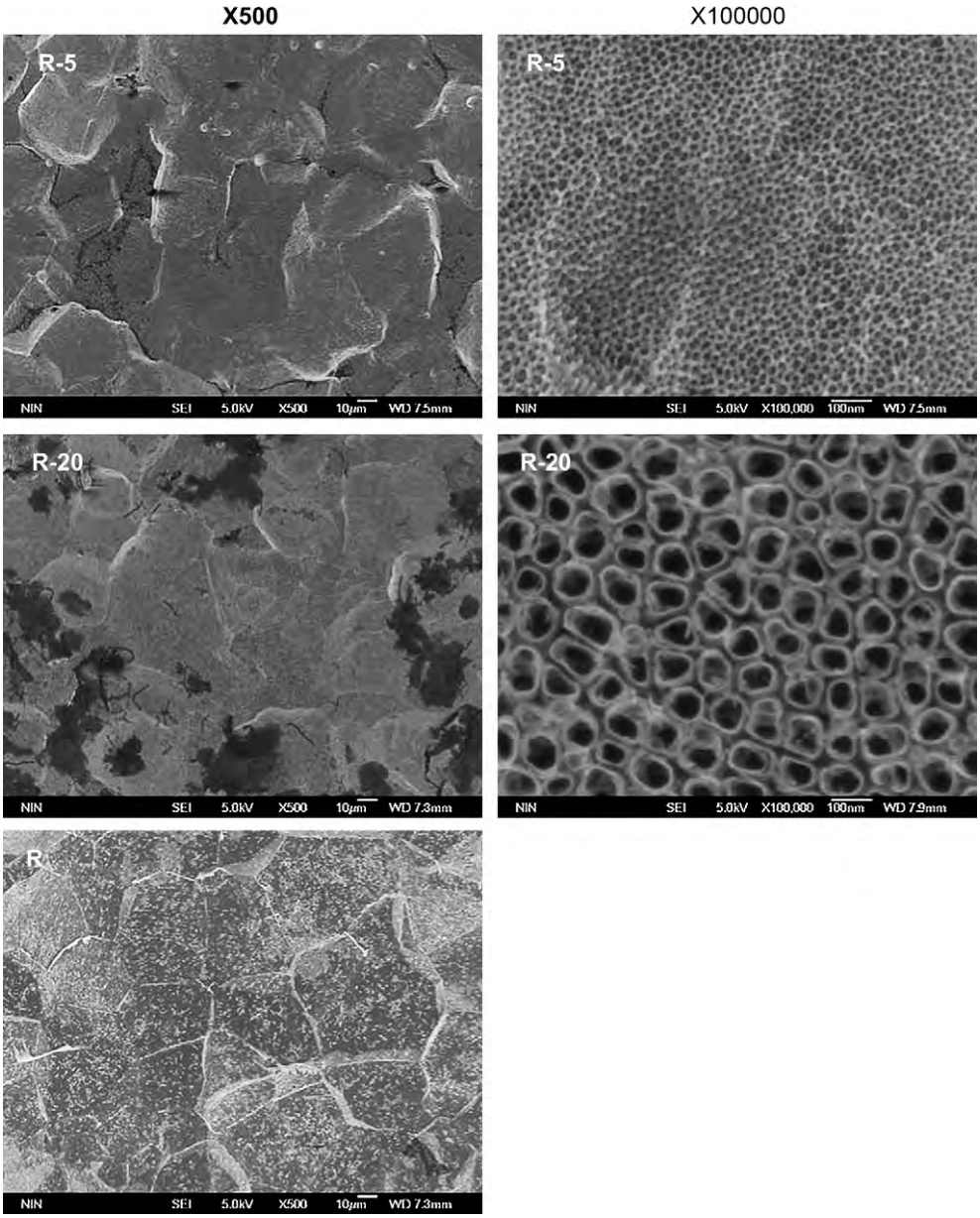

Fig. 1. SEM pictures of the hierarchical micro/nano-textured and micro titania surfaces. R-5: acid-etched/anodized at 5 V; R-20: acid-etched/anodized at 20 V; R: acid-etched microstructured surface.

3. Results

3.1. Fabrication of micro- and nanoscale titania surfaces

The nanotubular layers fabricated on the microstructured surface formed by acid etching are illustrated in Fig. 1. Micropits form initially on the titanium surface by etching in 0.5% HF acid. The surface structure consists of relatively sharp edges (Fig. 1C). After subsequent anodization, the sharp edges can be smoothed. Nanotubes of different sizes (diameters of about 15 and 80 nm) formed on the microstructured surface are distributed quite uniformly (Fig. 1A and B). According to the contact angle measurement and surface free energy calculation, the acid-etched microstructured surface has a slightly larger contact angle and a slightly lower surface energy than the smooth surface. The micro/nano-textured surface yields dramatically smaller water contact angles and bigger surface energy than both the microstructured and smooth surfaces (Table 1).

3.2. Protein adsorption

The amount of protein adsorbed on the surface from bovine calf serum after 4 h of incubation was assayed and the results are displayed in Fig. 2. More protein adsorbs on the acid-etched

Table 1
Contact angles (deg.) and values of surface free energy (mJ/m^2) of the various samples.

Samples	Contact angle (deg.)		Surface free energy (mJ/m^2)		
	Distilled water	Diiodomethane	Total	Polar	Disperse
R-5	16.22 ± 3.03	10.29 ± 3.23	78.81	28.82	49.99
R-20	21.67 ± 1.56	13.01 ± 1.74	76.90	27.39	49.50
R	70.51 ± 4.05	38.39 ± 2.34	47.39	6.98	40.41
S	63.90 ± 2.73	34.40 ± 2.78	51.83	9.53	42.30

R-5: acid-etched/anodized at 5 V; R-20: acid-etched/anodized at 20 V; R: acid-etched microstructured surface; S: smooth surface.

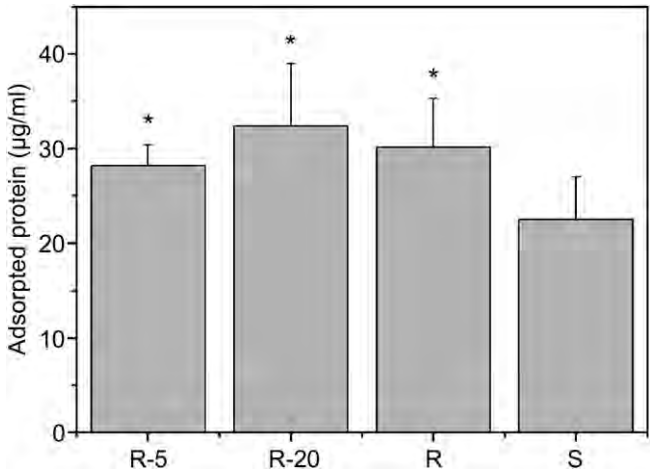

Fig. 2. Assay of protein adsorption to different specimens after 4 h of incubation in DMEM containing 10% bovine calf serum. R-5: acid-etched/anodized at 5 V; R-20: acid-etched/anodized at 20 V; R: acid-etched microstructured surface; S: smooth surface.

microstructured and micro/nano-textured surfaces than the smooth one, but there no appreciable difference in protein adsorption can be observed among the acid-etched micro-structured and micro/nano-textured surfaces.

3.3. Cytotoxicity assay

Cytotoxicity indicated by the LDH activity in the culture media after 24 h of incubation is compared in Fig. 3. After acid etching or acid etching and anodization, the samples show no obvious cytotoxicity compared to the smooth titanium and polystyrene culture dish as controls.

3.4. Cell adhesion

Cell adhesion on the specimens during the first 2 h of incubation is shown in Fig. 4. At each time interval adopted in this study, the adherent cell numbers on the acid-etched microstructured and micro/nano-textured surfaces are dramatically larger than that on the smooth surface. Then cell number on the acid-etched micro-structured surface is slightly higher than those on the micro/nano-textured surfaces after incubation for 30 and 120 min but the statistical difference is small. However, at 60 min, cell adhesion on the acid-etched microstructured surface is obviously higher than that on the micro/nano-textured surfaces with a statistical difference.

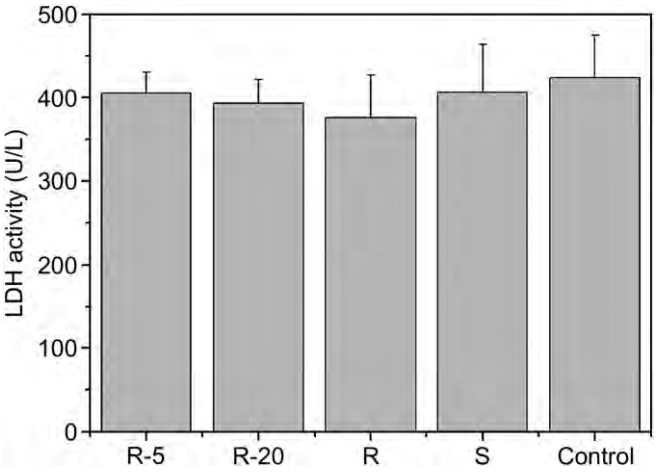

Fig. 3. Assay of LDH activity in the culture media after 24 h incubation of osteoblasts on the specimens. R-5: acid-etched/anodized at 5 V; R-20: acid-etched/anodized at 20 V; R: acid-etched microstructured surface; S: smooth surface.

3.5. Cell proliferation

Cell proliferation on the specimens during the first 7 days of incubation has been assessed and is illustrated in Fig. 5. There is no obvious difference among the samples at day 1. At day 4, the cell numbers on the micro/nano-textured surfaces are statistically lower than that on the smooth surface but the differences are quite small. After culturing for 7 days, the cell number on the acid-etched microstructured surface is statistically lower than that on the smooth surface, whereas those on the micro/nano-textured surfaces are higher than that on the acid-etched microstructured surface. The cell number on the acid-etched/20 V anodized surface is observed to be even slightly higher than that on the smooth surface.

3.6. Intracellular total protein content and alkaline phosphatase activity

The intracellular total protein synthesis and ALP activity after 7 days of culture have been measured and the results are exhibited in Fig. 6. The intracellular total protein content and ALP activity on the acid-etched microstructured surface are significantly depressed to about 40% and 20% relative to those on the smooth surface. Anodization dramatically enhances the intracellular total protein content and ALP activity. The intracellular total protein content on the acid-etched/5 V anodized surface and ALP activity on the acid-etched/20 V anodized surface are enhanced by about 30% relative to the smooth surface.

3.7. Collagen secretion

Collagen secretion quantified by the Sirius Red staining is shown in Fig. 7. According to the upper picture in Fig. 7, less collagen is secreted on the acid-etched microstructured surface compared to the smooth surface. However, on the micro/nano-textured surfaces, significantly denser collagen is deposited than both the acid-etched microstructured and the smooth surfaces, especially the acid-etched/20 V anodized surface. According to the quantitative results shown in Fig. 7, collagen deposition on the acid-etched micro-structured surface diminishes significantly by about 65% of that on the smooth surface. However, after anodization, collagen secretion is significantly promoted to about 115% and 125% on the acid-etched/5 V anodized and acid-etched/20 V anodized surfaces, respectively compared to the smooth one.

3.8. Extracellular matrix mineralization

Extracellular matrix mineralization measured by Alizarin Red staining is shown in Fig. 8. Extracellular matrix mineralization on the acid-etched microstructured surface is reduced but enhanced significantly after anodization. According to the quantitative results, matrix mineralization on the acid-etched microstructured surface is about 55% of that on the smooth surface. However, matrix mineralization on the micro/nano-textured surfaces is similar to that on the smooth surface.

3.9. Osteogenesis-related gene expressions

The gene expressions on the titania surfaces have been quantified using Real-time PCR as shown in Fig. 9. In general, gene expressions on the titania surfaces show a time dependent pattern. After 3 days of incubation, for the genes ITG, RUNX2 and OPN, the

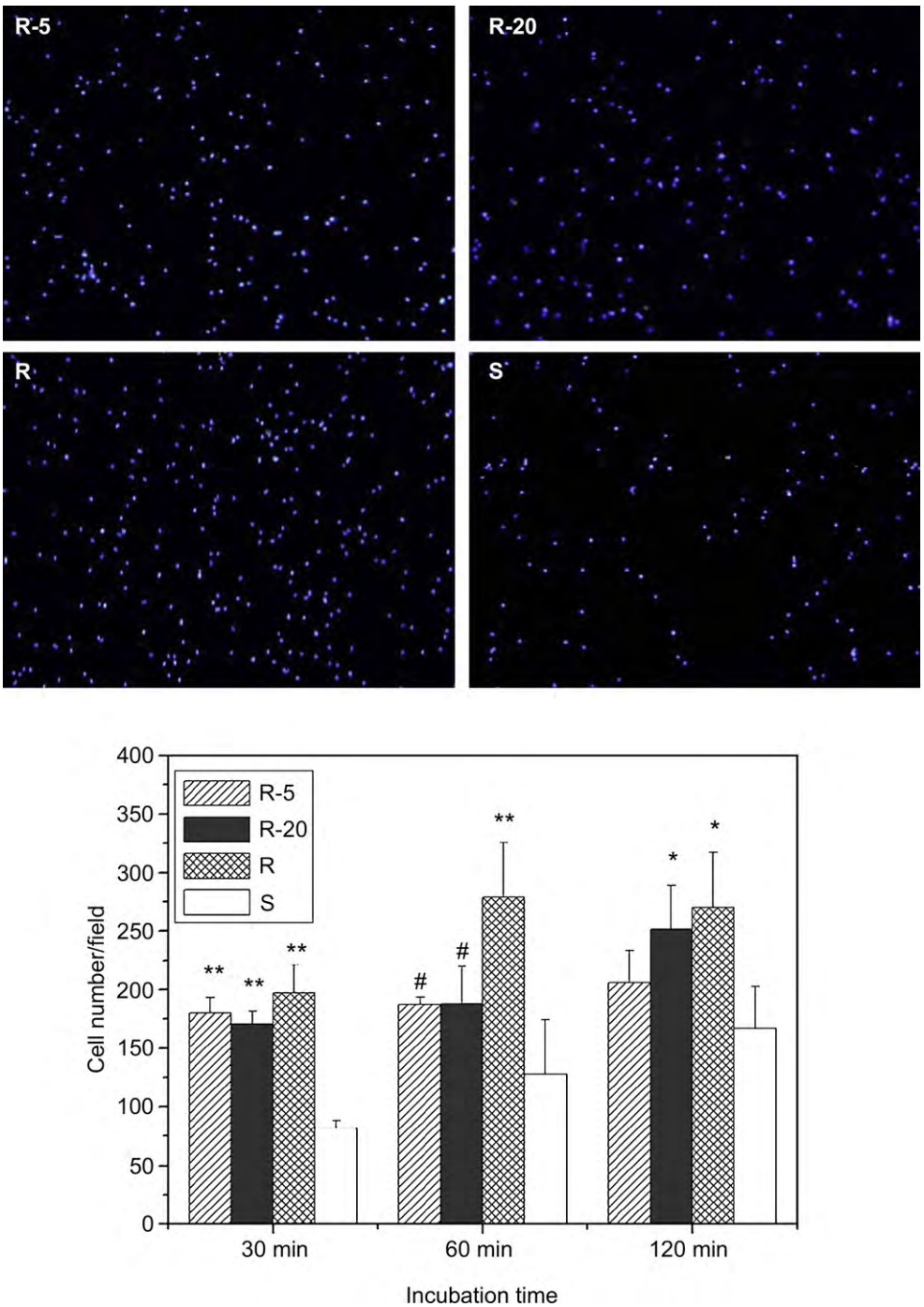

Fig. 4. Osteoblast adhesion measured by counting cells stained with DAPI under a fluorescence microscope after 30, 60 and 120 min of incubation. R-5: acid-etched/anodized at 5 V; R-20: acid-etched/anodized at 20 V; R: acid-etched microstructured surface; S: smooth surface. $^{*}p < 0.05$ and $^{**}p < 0.01$ compared with the smooth surface, $^{\#}p < 0.05$ compared with the acid-etched microstructured surface. The upper pictures show the fluorescence images of cells attached after 60 min of incubation.

smooth surface induces the highest expression followed by the acid-etched/20 V anodized surface. The acid-etched/5 V anodized surface and the acid-etched microstructured surface exhibits similar expression levels. For the genes ALP, BMP and OCN, the osteoblast expressions on the smooth surface, acid-etched microstructured surface, and acid-etched/20 V anodized surface are similar, but the expressions on the acid-etched/5 V anodized surface are dramatically lower. After culturing for 10 days, the acid-etched microstructured surface yields higher expressions for all genes assayed in this study compared to the other surfaces even though no statistical difference can be found for genes RUNX2 and OPN. Gene expressions on the other three surfaces show no obvious difference except that the expressions of ITG on the acid-etched/20 V anodized surface and OCN on the acid-etched/5 V anodized surface are higher than those on the other two surfaces.

4. Discussion

Hierarchical hybrid micro/nano-textured surface topographies are produced on titanium using common and easy acid etching

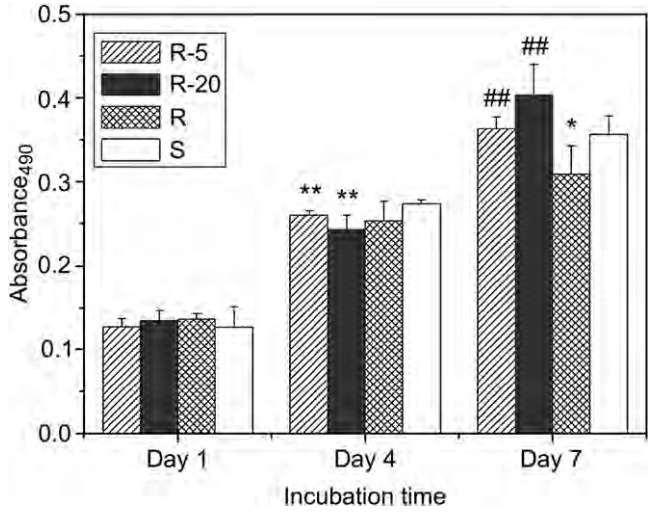

Fig. 5. Cell proliferation on samples after 1, 4 and 7 days of incubation measured by colorimetric MTT assay. R-5: acid-etched/anodized at 5 V; R-20: acid-etched/anodized at 20 V; R: acid-etched microstructured surface; S: smooth surface. $^{*}p < 0.05$ and $^{**}p < 0.01$ compared with the smooth surface, $^{\#\#}p < 0.01$ compared with the acid-etched microstructured surface.

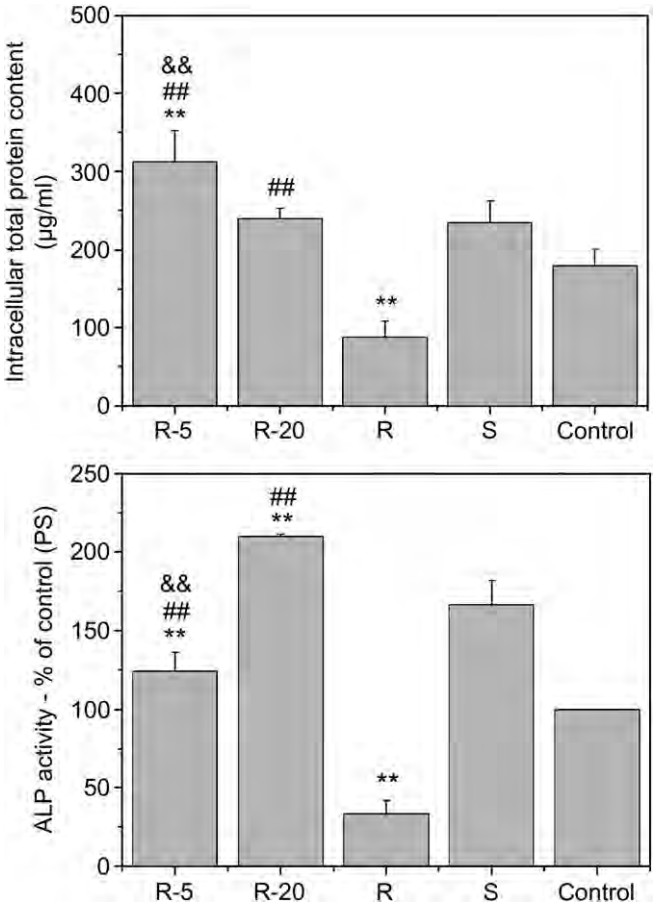

Fig. 6. Intracellular total protein synthesis (upper panel) and ALP activity (lower panel) of osteoblasts on samples after 7 days of incubation. R-5: acid-etched/anodized at 5 V; R-20: acid-etched/anodized at 20 V; R: acid-etched microstructured surface; S: smooth surface. $^{**}p < 0.01$ compared with the smooth surface, $^{\#\#}p < 0.01$ compared to the acid-etched microstructured surface, $^{\&\&}p < 0.01$ compared with the acid-etched/20 V anodized surface.

combined with anodization and the micro/nano-textured surface structures are illustrated to induce different biological reactions from primary osteoblasts. Though the microtopography formed by acid etching induces higher initial cell adhesion and osteogenesis-related gene expressions, other cell behaviors such as proliferation, intracellular total protein synthesis and ALP activity, extracellular matrix deposition and mineralization are significantly reduced. After addition of nanotubes to the micropitted surface, even though cell adhesion and gene expressions decrease slightly compared to the microtopography, other cell functions such as proliferation, intracellular total protein synthesis and ALP activity, extracellular matrix deposition, and mineralization are maintained or enhanced. Our results suggest that the micro/nano-textured surface topographies may be more biologically friendly rendering more balanced promotion in multiple cell functions.

A microtopography is widely believed to benefit bone implant osseointegration and some of the developed technologies have been adopted commercially although problems still exist [2–7]. The most important issue is to balance the dilemma between cell proliferation and cell differentiation and to enhance both of them simultaneously. Higher cell proliferation results in more cell colonization on the implant surface probably leading to a larger mass of bone tissue around the implant. On the other hand, faster cell differentiation may result in faster bone maturation around the implant and offer more promise in bone implant bonding. Biomaterial surfaces with microscale roughness are effective in promoting osteoblast differentiation [8–10,12], but they depress osteoblast proliferation [9–12] leading to a smaller bone mass around them compared to a smooth surface. In this study, similar results have been observed. Higher cell adhesion and gene expressions are found on the acid-etched microstructured surface, while other cell functions such as proliferation, intracellular total protein synthesis and ALP activity, extracellular matrix deposition and mineralization are significantly reduced. The reasons why the intracellular total protein synthesis and ALP activity, extracellular matrix deposition and mineralization are depressed on the acid-etched microstructured surface although some osteogenesis-related gene expressions are dramatically enhanced are still not clear. It cannot be explained solely by reduced cell proliferation because cell proliferation is not severely compromised. It is supposed that the hampered cell–cell communication may partly account for those depressed cell functions. Cell–cell communication is reported to be very important to cell function development, coordinating cellular responses to external signals, and regulating osteoblast differentiation [44–47]. Cells on the acid-etched microstructured surface may not make good direct cell–cell communication because of the low cell population and its relatively larger surface area. The low cell population combined with hampered cell–cell communication may constitute a better explanation for the lower intracellular total protein synthesis, ALP activity, as well as extracellular matrix deposition and mineralization on the acid-etched microstructured surface, but more study is needed to elucidate the mechanism in details.

This study reveals that addition of nanotubes to the microstructured surface leads to more balanced enhancement of multiple cell functions. Though initial cell adhesion and gene expressions are slightly depressed on the hybrid micro/nano-textured surfaces compared to the acid-etched microstructured surface, other cell functions investigated in this study are significantly enhanced, and some of them are even much higher than those on the smooth surface. The hybrid micropit-and-nanonodule surface structure developed by Kubo et al. also induces simultaneous enhancement of osteoblast proliferation and differentiation compared to the micropit surface [39]. Compared to the microtopography, the balanced enhancement of multiple cell functions on the hierarchical micro/nano-textured surface may lead to faster bone

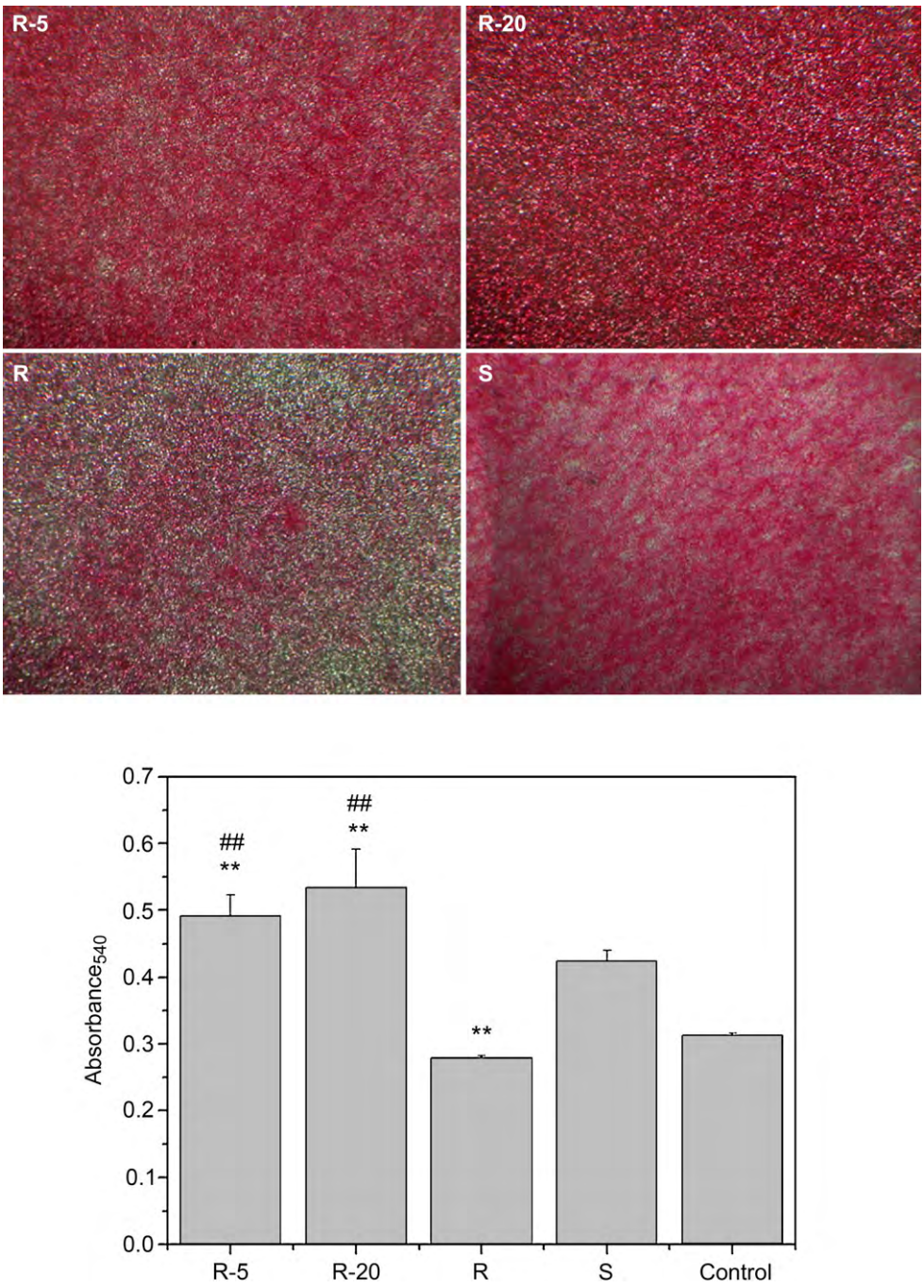

Fig. 7. Collagen secretion by osteoblasts on the samples after 7 days of incubation: optical images (upper panel) and colorimetrically quantitative analysis (lower panel). R-5: acid-etched/anodized at 5 V; R-20: acid-etched/anodized at 20 V; R: acid-etched microstructured surface; S: smooth surface. $^{**}p < 0.01$ compared with the smooth surface, $^{\#\#}p < 0.01$ compared to the acid-etched microstructured surface.

maturation around the implant without compromising the bone mass. Besides, the mechanical interlocking ability of the microtopography is maintained in this micro/nanostructure. Hence, the hierarchical micro/nanostructure described here may lead to a better implant osseointegration *in vivo*. It is noticed in our experiments that the microtopography itself is not altered too much after anodization, except that the sharp edges become blunt. This minor change is not expected to give rise to such dramatically different biological response. Therefore, it can be inferred that the changes are caused by the addition of nanotubes. The amount of protein adsorption does not appear to be the main reason why the micro/nano-textured surfaces enhance cell functions as anodization does not enhance the amount of protein adsorption. Assay of the selective protein adsorption property of specimens may provide better explanation because some specific protein such as fibronectin or laminin is suggested to play a more vital role in cell/biomaterial interactions. In addition, the conformation of the adsorbed protein is also important.

We have previously observed equal or slightly reduced cell proliferation on anodized nanotopographies (unpublished data). A microtopography is known to promote osteoblast differentiation but reduce osteoblast proliferation [8–11]. Thus, it is proposed that

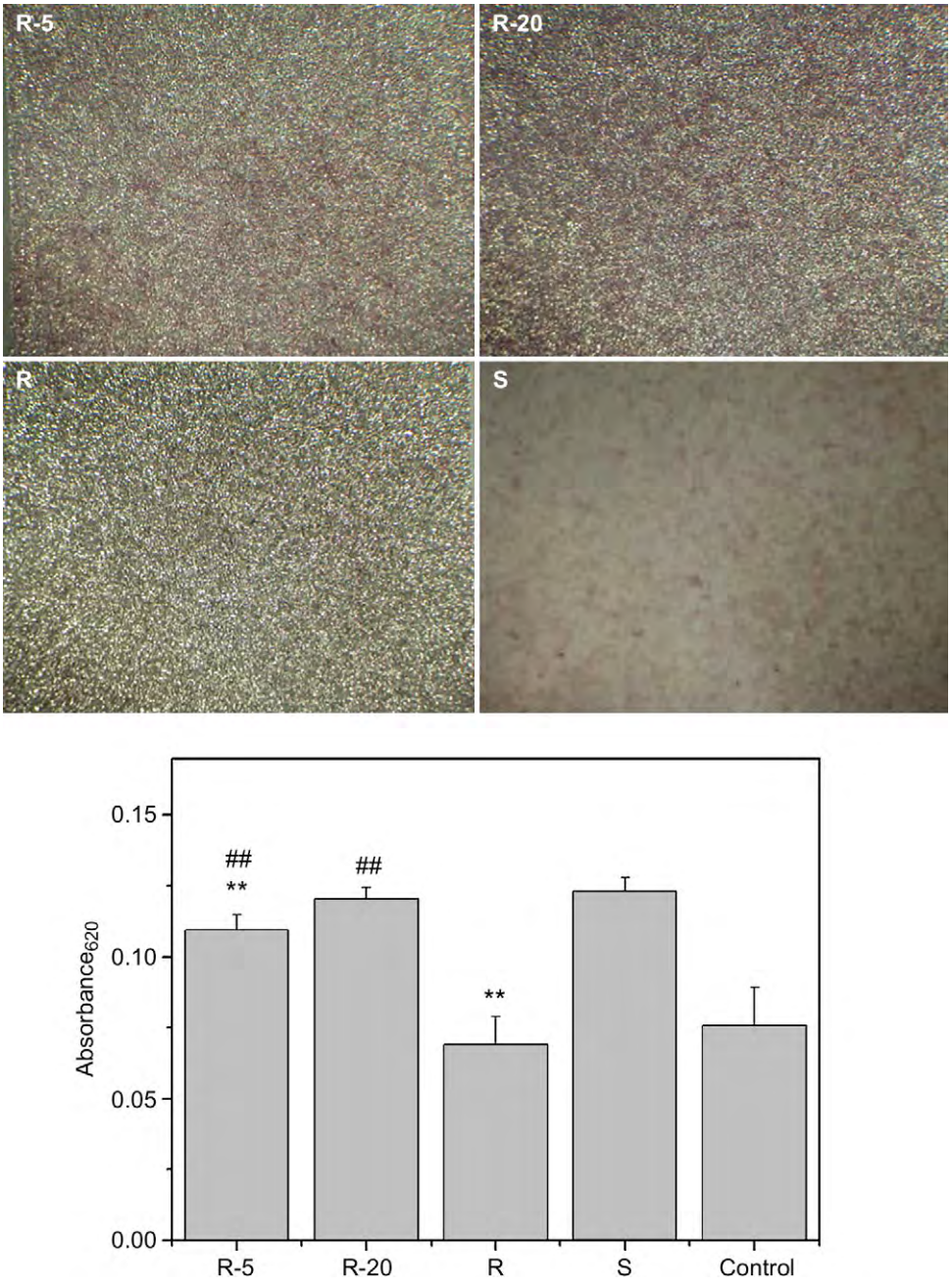

Fig. 8. Extracellular matrix mineralization on samples after 7 days of incubation: optical images (upper panel) and colorimetrically quantitative analysis (lower panel). R-5: acid-etched/anodized at 5 V; R-20: acid-etched/anodized at 20 V; R: acid-etched microstructured surface; S: smooth surface. $^{**}p < 0.01$ compared with the smooth surface, $^{\#\#}p < 0.01$ compared with the acid-etched microstructured surface.

the unaffected or slightly enhanced osteoblast proliferation on the micro/nano-textured surfaces is probably due to a synergistic effect rendered by the micro and nanotopography. Zinger et al. have suggested that the micro and submicrotopography may play a synergistic role in osteoblast proliferation [41]. With regard to the intracellular total protein synthesis and alkaline phosphatase activity, a synergistic effect is also suggested. The intracellular total protein synthesis and alkaline phosphatase activity on the acid-etched microstructured surface are about 40% and 20% of those on the smooth surface, respectively (Fig. 6). On the surfaces with only nanotexture, intracellular total protein synthesis was a little lower than that on the smooth surface, and on the 20 V anodized nano-textured surface, the alkaline phosphatase activity was a little higher than that on the smooth surface [43]. Nevertheless, addition of nanotubes to the acid-etched microstructured surface induces dramatic increase in these two parameters which are even higher than those observed from the smooth control (Fig. 6). This may be the first evidence demonstrating the synergistic effects of the micro and nanotopography on osteoblast behavior.

Collagen secretion and extracellular matrix mineralization are also enhanced by the addition of nanotubes to the microstructured Ti surface. Enhancement of these two parameters can be ascribed to the nanotubes. Nanotubes were observed to dramatically increase collagen secretion and extracellular matrix mineralization in our previous study [43]. However, the synergistic contributions by the micro and nanotopography on collagen secretion must be taken

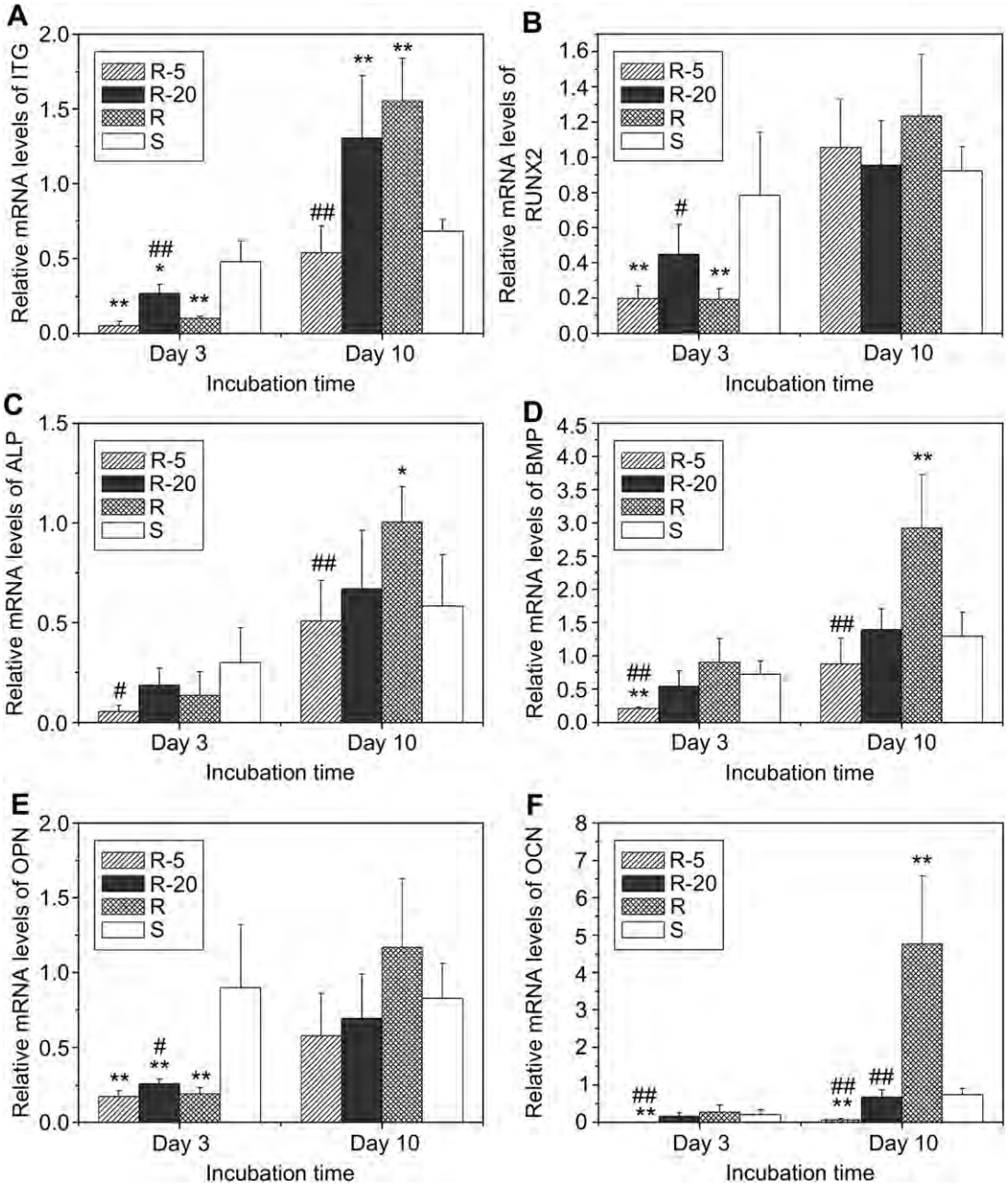

Fig. 9. Gene expressions by primary osteoblasts cultured on titanium surfaces after incubation of 3 and 10 days: (A) Integrin-β1, (B) RUNX2, (C) ALP, (D) BMP, (E) osteopontin and (F) osteocalcin. The data are generated by Real-time PCR and are shown as mean expression relative to GAPDH ± SD. R-5: acid-etched/anodized at 5 V; R-20: acid-etched/anodized at 20 V; R: acid-etched microstructured surface; S: smooth surface. $^{*}p < 0.05$ and $^{**}p < 0.01$ compared with the smooth surface, $^{\#}p < 0.05$ and $^{\#\#}p < 0.01$ compared to the acid-etched microstructured surface.

into account, because 5 V and 20 V anodization enhanced collagen secretion by about 65% and 70% relative to the smooth surface [43] whereas addition of 5 V and 20 V nanotubes to the microstructured surface increases it by about 75% and 90% relative to the microstructured surface alone (Fig. 7).

The biological performance of titania nanotubes is still not well understood and conflicting results have been reported. In our previous study, we showed that the phenotype of cells used (unpublished data) and sterilization process used on titania nanotubes [43] influenced their biological behaviors. This study indicates that the microstructured surface with an added nano element by introducing nanotubes also influences the cytocompatibility of titania nantubes. The hierarchical micro/nano-textured topography reported here may provides insight to future development of titanium implants. Addition of nanotubes to the microstructured surface can broadly promotes cell functions. The simultaneous enhancement of cell adhesion, proliferation, intracellular total protein synthesis, alkaline phosphatase activity, and collagen secretion may lead to faster bone maturation around the implant without compromising the bone mass, probably inducing better osseointegration. Moreover, the fabrication method reported here is easy, inexpensive, is easily adoptable by the biomedical industry. This hierarchical micro/nano-textured surface topography may also provide a platform to investigate cell/implant interaction and to further optimize the matching between the micro and nano textures to yield better bioactivity.

5. Conclusion

Hierarchical hybrid micro/nano-textured surfaces have been produced by acid etching and anodization. The microtexture produced by acid etching induces inconsistent osteoblast functions with initial cell adhesion and osteogenesis-related gene expressions dramatically enhanced while other cell behaviors such as proliferation, intracellular total protein synthesis and alkaline phosphatase activity, and extracellular matrix deposition and mineralization are significantly depressed. Addition of nanotubes to the microstructured surface enhances multiple osteoblast behaviors with nearly all the cell functions studied here retained or promoted. This hierarchical micro/nano-textured surface topography may result in better osseointegration *in vivo*. Our study reveals the synergistic role played by the micro and nano-topographies on osteoblast functions and provides insight to future implant surface design.

Acknowledgements

This work was supported by the National Natural Science Foundation of China No. 30672347 and Hong Kong Research Grants Council (RGC) General Research Fund (GRF) No. CityU 112307.

Appendix

Figures with essential color discrimination. Figs. 4, 7, 8 in this article are difficult to interpret in black and white. The full color images can be found in the online version, at doi:10.1016/j.biomaterials.2010.03.014.

References

[1] Anselme K. Osteoblast adhesion on biomaterials. Biomaterials 2000;21:667–81.
[2] Hansson S, Norton M. The relation between surface roughness and interfacial shear strength for bone-anchored implants. A mathematical model. J Biomech 1999;32:829–36.
[3] Schwartz Z, Nasazky E, Boyan BD. Surface microtopography regulates osteointegration: the role of implant surface microtopography in osteointegration. Alpha Omegan 2005;98:9–19.
[4] Zhao L, Wei Y, Li J, Han Y, Ye R, Zhang Y. Initial osteoblast functions on Ti-5Zr-3Sn-5Mo-15Nb titanium alloy surfaces modified by microarc oxidation. J Biomed Mater Res A 2010;92A:432–40.
[5] Lamolle SF, Monjo M, Rubert M, Haugen HJ, Lyngstadaas SP, Ellingsen JE. The effect of hydrofluoric acid treatment of titanium surface on nanostructural and chemical changes and the growth of MC3T3-E1 cells. Biomaterials 2009;30:736–42.
[6] Monjo M, Lamolle SF, Lyngstadaas SP, Ronold HJ, Ellingsen JE. In vivo expression of osteogenic markers and bone mineral density at the surface of fluoride-modified titanium implants. Biomaterials 2008;29:3771–80.
[7] Guo J, Padilla RJ, Ambrose W, De Kok IJ, Cooper LF. The effect of hydrofluoric acid treatment of TiO_2 grit blasted titanium implants on adherent osteoblast gene expression in vitro and in vivo. Biomaterials 2007;28:5418–25.
[8] Kim MJ, Kim CW, Lim YJ, Heo SJ. Microrough titanium surface affects biologic response in MG63 osteoblast-like cells. J Biomed Mater Res A 2006;79:1023–32.
[9] Lohmann CH, Bonewald LF, Sisk MA, Sylvia VL, Cochran DL, Dean DD, et al. Maturation state determines the response of osteogenic cells to surface roughness and 1,25-dihydroxyvitamin D3. J Bone Miner Res 2000;15:1169–80.
[10] Boyan BD, Lossdörfer S, Wang L, Zhao G, Lohmann CH, Cochran DL, et al. Osteoblasts generate an osteogenic microenvironment when grown on surfaces with rough microtopographies. Eur Cell Mater 2003;6:22–7.
[11] Saito T, Hayashi H, Kameyama T, Hishida M, Nagai K, Teraoka K, et al. Suppressed proliferation of mouse osteoblast-like cells by a rough-surfaced substrate leads to low differentiation and mineralization. Mater Sci Eng C 2010;30:1–7.
[12] Schwartz Z, Olivares-Navarrete R, Wieland M, Cochran DL, Boyan BD. Mechanisms regulating increased production of osteoprotegerin by osteoblasts cultured on microstructured titanium surfaces. Biomaterials 2009;30:3390–6.
[13] Liu H, Webster TJ. Nanomedicine for implants: a review of studies and necessary experimental tools. Biomaterials 2006;28:354–69.
[14] Bjursten LM, Rasmusson L, Oh S, Smith GC, Brammer KS, Jin S. Titanium dioxide nanotubes enhance bone bonding in vivo. J Biomed Mater Res A 2010;92:1218–24.
[15] Eaninwene 2nd G, Yao C, Webster TJ. Enhanced osteoblast adhesion to drug-coated anodized nanotubular titanium surfaces. Int J Nanomedicine 2008;3:257–64.
[16] Oh S, Daraio C, Chen LH, Pisanic TR, Finones RR, Jin S. Significantly accelerated osteoblast cell growth on aligned TiO_2 nanotubes. J Biomed Mater Res A 2006;78A:97–103.
[17] Park J, Bauer S, von der Mark K, Schmuki P. Nanosize and vitality: TiO_2 nanotube diameter directs cell fate. Nano Lett 2007;7:1686–91.
[18] Popat KC, Eltgroth M, La Tempa TJ, Grimes CA, Desai TA. Titania nanotubes: a novel platform for drug-eluting coatings for medical implants? Small 2007;3:1878–81.
[19] Popat KC, Eltgroth M, Latempa TJ, Grimes CA, Desai TA. Decreased Staphylococcus epidermis adhesion and increased osteoblast functionality on antibiotic-loaded titania nanotubes. Biomaterials 2007;28:4880–8.
[20] Brammer KS, Oh S, Cobb CJ, Bjursten LM, van der Heyde H, Jin S. Improved bone-forming functionality on diameter-controlled TiO_2 nanotube surface. Acta Biomater 2009;5:3215–23.
[21] Park J, Bauer S, Schmuki P, von der Mark K. Narrow window in nanoscale dependent activation of endothelial cell growth and differentiation on TiO_2 nanotube surfaces. Nano Lett 2009;9:3157–64.
[22] Park J, Bauer S, Schlegel KA, Neukam FW, von der Mark K, Schmuki P. TiO_2 nanotube surfaces: 15 nm—an optimal length scale of surface topography for cell adhesion and differentiation. Small 2009;5:666–71.
[23] Brammer KS, Oh S, Gallagher JO, Jin S. Enhanced cellular mobility guided by TiO_2 nanotube surfaces. Nano Lett 2008;8:786–93.
[24] Das K, Bose S, Bandyopadhyay A. TiO_2 nanotubes on Ti: influence of nanoscale morphology on bone cell-materials interaction. J Biomed Mater Res A 2009;90:225–37.
[25] Popat KC, Leoni L, Grimes CA, Desai TA. Influence of engineered titania nanotubular surfaces on bone cells. Biomaterials 2007;28:3188–97.
[26] Oh S, Brammer KS, Li YS, Teng D, Engler AJ, Chien S, et al. Stem cell fate dictated solely by altered nanotube dimension. Proc Natl Acad Sci U S A 2009;106:2130–5.
[27] Yao C, Slamovich EB, Webster TJ. Enhanced osteoblast functions on anodized titanium with nanotube-like structures. J Biomed Mater Res A 2008;85:157–66.
[28] Peng L, Eltgroth ML, LaTempa TJ, Grimes CA, Desai TA. The effect of TiO_2 nanotubes on endothelial function and smooth muscle proliferation. Biomaterials 2009;30:1268–72.
[29] Burns K, Yao C, Webster TJ. Increased chondrocyte adhesion on nanotubular anodized titanium. J Biomed Mater Res A 2009;88:561–8.
[30] Balasundaram G, Yao C, Webster TJ. TiO_2 nanotubes functionalized with regions of bone morphogenetic protein-2 increases osteoblast adhesion. J Biomed Mater Res A 2008;84:447–53.
[31] Peng L, Mendelsohn AD, LaTempa TJ, Yoriya S, Grimes CA, Desai TA. Long-term small molecule and protein elution from TiO_2 nanotubes. Nano Lett 2009;9:1932–6.
[32] Song YY, Schmidt-Stein F, Bauer S, Schmuki P. Amphiphilic TiO_2 nanotube arrays: an actively controllable drug delivery system. J Am Chem Soc 2009;131:4230–2.
[33] Shrestha NK, Macak JM, Schmidt-Stein F, Hahn R, Mierke CT, Fabry B, et al. Magnetically guided titania nanotubes for site-selective photocatalysis and drug release. Angew Chem Int Ed Engl 2009;48:969–72.
[34] Rho JY, Kuhn-Spearing L, Zioupos P. Mechanical properties and the hierarchical structure of bone. Med Eng Phys 1998;20:92–102.
[35] Santos MI, Unger RE, Sousa RA, Reis RL, Kirkpatrick CJ. Crosstalk between osteoblasts and endothelial cells co-cultured on a polycaprolactone-starch scaffold and the in vitro development of vascularization. Biomaterials 2009;30:4407–15.
[36] Santos MI, Tuzlakoglu K, Fuchs S, Gomes ME, Peters K, Unger RE, et al. Endothelial cell colonization and angiogenic potential of combined nano- and micro-fibrous scaffolds for bone tissue engineering. Biomaterials 2008;29:4306–13.
[37] Tan J, Saltzman WM. Biomaterials with hierarchically defined micro- and nanoscale structure. Biomaterials 2004;25:3593–601.
[38] George PA, Quinn K, Cooper-White JJ. Hierarchical scaffolds via combined macro- and micro-phase separation. Biomaterials 2010;31:641–7.
[39] Kubo K, Tsukimura N, Iwasa F, Ueno T, Saruwatari L, Aita H, et al. Cellular behavior on TiO_2 nanonodular structures in a micro-to-nanoscale hierarchy model. Biomaterials 2009;30:5319–29.
[40] Gao L, Feng B, Wang J, Lu X, Liu D, Qu S, et al. Micro/nanostructural porous surface on titanium and bioactivity. J Biomed Mater Res B Appl Biomater 2009;89B:335–41.
[41] Zinger O, Anselme K, Denzer A, Habersetzer P, Wieland M, Jeanfils J, et al. Time-dependent morphology and adhesion of osteoblastic cells on titanium model surfaces featuring scale-resolved topography. Biomaterials 2004;25:2695–711.
[42] Fan H, Chen P, Qi R, Zhai J, Wang J, Chen L, et al. Greatly improved blood compatibility by microscopic multiscale design of surface architectures. Small 2009;5:2144–8.
[43] Zhao L, Mei S, Wang W, Chu PK, Wu Z, Zhang Y. The role of sterilization in the cytocompatibility of titania nanotubes. Biomaterials 2010;31:2055–63.
[44] Schiller PC, D'Ippolito G, Balkan W, Roos BA, Howard GA. Gap-junctional communication mediates parathyroid hormone stimulation of mineralization in osteoblastic cultures. Bone 2001;28:38–44.

[45] Gramsch B, Gabriel HD, Wiemann M, Grummer R, Winterhager E, Bingmann D, et al. Enhancement of connexin 43 expression increases proliferation and differentiation of an osteoblast-like cell line. Exp Cell Res 2001; 264:397–407.
[46] Marie PJ. Role of N-cadherin in bone formation. J Cell Physiol 2002;190: 297–305.
[47] Civitelli R. Cell-cell communication in the osteoblast/osteocyte lineage. Arch Biochem Biophys 2008;473:188–92.